COMPARISON OF ESCAPE RATES FOR A VACANCY DIFFUSION THROUGH ONE--JUMP AND SIX--JUMP CYCLES IN WELL ORDERED BINARY ALLOYS.

A Thesis Submitted to the School of Graduate Studies
Addis Ababa University

In partial Fulfilment of the Requirements for the
Degree of Master of Science in Physics

By

Alemayehu Kasahun

Addis Ababa, Ethiopia
July 2006.

ADDIS ABABA UNIVERSITY
FACULTY OF SCIENCE
DEPARTMENT OF PHYSICS

The undersigned hereby certify that they have read and recommended to the Faculty of Science School of Graduate Studies for acceptance a thesis entitled "**COMPARISON OF ESCAPE RATES FOR A VACANCY DIFFUSION THROUGH ONE--JUMP AND SIX--JUMP CYCLES IN WELL ORDERED BINARY ALLOYS.** " by **Alemayehu Kasahun** in partial fulfillment of the requirements for the degree of **Master of Science in Physics**.

July 2006

Name	Signature
Dr. Mulugeta Bekele, Advisor	_____
Dr. Mesfin Asfaw, Examiner	_____
Dr. S. K. Ghoshal, Examiner	_____

To my family.

Acknowledgements

Above all, I would like to thank the Almighty God for his timely endowment. With deep sense of gratitude, I would like to express my sincere thanks to my advisor and instructor Dr. Mulugeta Bekele who kept eyes in guiding, assisting, supervising and contributing invaluable suggestion as final words during the course of work greatly acknowledge. His scientific excitement, integral view on research and overly enthusiasm, has made a deep impression on me. I owe him lots of gratitude for having me shown this way of research.

I wish to express my warm and sincere thanks to Dr. Mesfin Asfaw for his valuable comments and suggestion.

It is a pleasant aspect that I have now the opportunity to express my deepest gratitude to my family. Thank you does not seem sufficient for them but it is said with appreciation and respect. They rendered me enormous support, stimulating suggestions, encouragement and taught of hard work by their own example. This journey will not be easy without them. I would like to thank them once again.

Lastly, I would like to thank all whose direct and indirect support helped me to complete my thesis on time.

Addis Ababa, Ethiopia — Alemayehu Kasahun
July 2006.

Abstract

We use a Supersymmetry Quantum Mechanics method to calculate the escape rate of vacancy diffusion in well ordered binary alloy for low concentration structural defect in two dimension. The dynamics was mediated by long range and short range one atom and vacancy exchange. We examine the ratio of escape rate for the six-jump cycle to that for the one-jump cycle. When the effective barrier height of the six-jump cycle is greater than or equal that of the one-jump cycle, the escape rate for the one-jump cycle is larger than that of the six-jump cycle. If the effective barrier height of the six-jump cycle is less than that of the one-jump cycle, for relatively high temperature the escape rate for the one-jump cycle is higher than that of the six-jump cycle but at relatively low temperature the reverse is observed. We have also seen that at a ceratin temperature or barrier height, both the six-jump and the one-jump cycles have equal escape rates.

Table of Contents

Table of Contents vi

List of Figures vii

1 Introduction 2

2 The Dynamics for Motion of Vacany and Supersymmetric Quantum Mechanics 7
- 2.1 The Dynamics for Vacancy Motion 7
- 2.2 Supersymmetric Quantum Mechanics 10

3 The Energy Configuration and Calculation of Escape Rate for One-Jump and Six-Jump Cycles 15
- 3.1 One-Jump Cycle 15
  - 3.1.1 The Energy Configuration for One-Jump Cycle 15
  - 3.1.2 Calculation of Escape Rate for Direct Jump 18
- 3.2 Six-Jump Cycle 24
  - 3.2.1 The Energy Configuration for Six-Jump 24
  - 3.2.2 Calculation of Escape Rate for Six-Jump 28

4 Result and Discussion 36

5 Summary and Conclusion 45

A Derivation for Elements of the Matrix T Cubed 47

Bibliography 51

List of Figures

1.1 Diagram for well ordered binary alloy (B2 structure), A and B, with a vacancy placed at site A'. 4

2.1 Generalized ladder operators of supersymmetric potential that connects states of the same energy. 14

3.1 (I) The one-jump in B2 compounds. (II) Schematic picture of the energy change during one-jump cycle. 16

3.2 (I) The model potential U(x) versus x. (II) Plot of V_ (x) versus x (not scaled). 17

3.3 : (I) The six-jump cycles in the B2 structure. (II) A schematic picture of the energy changes of the system during the course of cycle. 24

3.4 (I) The model potential U(x) versus x. (II) Plot of $V_{-}(x)$ versus x (not scaled). (III) A figure showing a step of the subdivided potential found between the intervals x_n and x_{n+1}. 26

4.1 Plots of R_{61} versus $\frac{U_1}{2k_BT}$ for $m = 0.8$. 37

4.2 Plots of R_{61} versus $\frac{U_1}{2k_BT}$ for $m = 1$. 38

4.3 Plots of R_{61} versus $\frac{U_1}{2k_BT}$ for $m = 1.2$. 39

4.4 Plots of R_{61} versus $\frac{U_1}{2k_BT}$ for $m = 1.4$. 40

4.5 Plots of R_{61} versus $\frac{U_1}{2k_BT}$ for $m = 1.6$. 41

4.6 Plots of R_{61} versus m for $\frac{U_1}{2k_BT} = 0.8$. 42

4.7 Plots of R_{61} versus m for $\frac{U_1}{2k_BT} = 1$. 43

4.8 Plots of R_{61} versus m for $\frac{U_1}{2k_BT} = 1.2$. 43
4.9 Plots of R_{61} versus m for $\frac{U_1}{2k_BT} = 1.4$. 44

Chapter 1

Introduction

Real crystals are not perfect; they always contain a considerable density of defects and imperfection that affect their physical, chemical, mechanical and electronic properties. Defects do not necessarily have adverse effect on the properties of materials. There are many situations in which a judicious control of the types and amounts of imperfections can bring about a specific characteristics desired in a system. Different kinds of defects in a solid can be conveniently classified into four categories: point defect (atom is missing or placed in irregular places in the lattice), line defect(group of atoms in irregular position), planar defect or grain boundaries or interfacial defect(the interfaces between homogeneous regions of the material (grain boundaries, external surfaces)) and bulk or volume defect(extended defects(pores, cracks)).

Two types of point defects are inherent to the equilibrium state, namely, vacancy and self-interstitial. They are determined by temperature, pressure and composition of a given system. The presence and concentration of other defects, however, depend on the way the solid was originally formed and subsequently processed.

Vacancies are point defects of size nearly equivalent to the size of the original (occupied) site. The probability that a given site is vacant is proportional to the

Boltzmann factor for the system in equilibrium is $P = exp\left(\frac{-E_v}{k_B T}\right)$ [1], where E_v is the energy required to take an atom from a lattice site inside the crystal to a lattice on the surface.

In many crystalline material the elementary process of diffusion commonly takes place through the site exchange between a vacancy and neighboring atom. In pure metals self diffusion occurs by random motion of vacancies. In ordered alloys or compounds, however, random vacancy motion is not possible as it would disrupt the equilibrium ordered arrangement of atoms on lattice sites. During this exchange, the moving atom must pass through a state of high energy. This creates energy barrier for atomic motion. The ordered atomic structure of intermetallic compounds, say A-B materials consist of two interpenetrating simple cubic or square sublattices which are predominantly occupied by two different atoms A and B, imposes some restrictions on diffusion mechanisms because the various constituent atoms are preferentially located at various sublattice. Hence the exchange of the vacancy with the nearest-neighbor atom is associated with local disturbance of the, A-B, ordering. At low temperature, for example this implies an additional energetic barrier against diffusion in well-ordered alloys.

In view of this limitation, two alternative types of diffusion mechanisms are conceivable to avoid these problems (see, for instance, [2]), either jumps of vacancies to further distant site on the same sublattice or cycles of nearest-neighbor jumps in such a way that the atomic disorder appearing during the intermediate states of the cycle is repaired when the cycle is completed. The most prominent proposed mechanism is a six-jump cyclic mechanism of vacancy movement that gives a solution by retaining the atomic order, which might overcome the barrier without altering the long-range

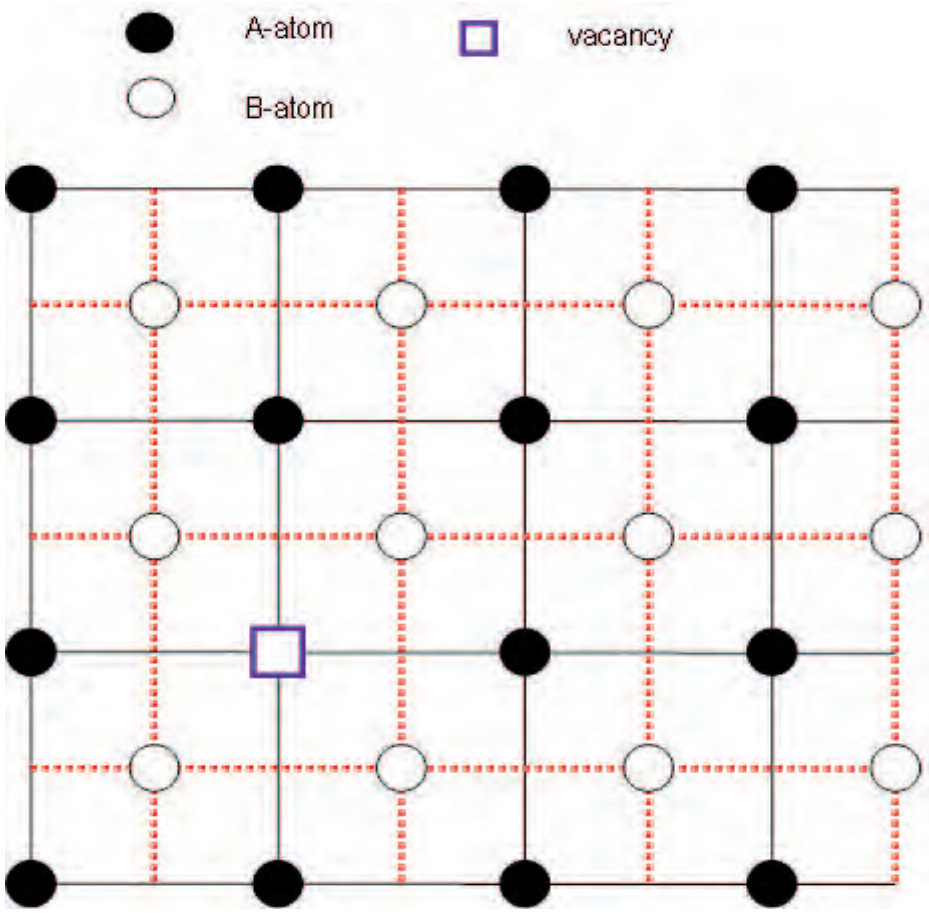

Figure 1.1: Diagram for well ordered binary alloy (B2 structure), A and B, with a vacancy placed at site A'.

order. It was proposed for the intermetallic compounds with $B2$ structure at low temperature by Elcock and McCombie[3]. In order for the vacancy to execute any other non-trivial series of jumps starting from its most stable state and end on its other most stable state, it must pass through higher energy configuration than any occurring in the six-jump process[3].

Next we consider a vacancy jump through perfectly well ordered AB lattice in two

dimensions. An alloy with two sublattices interpenetrating each other such that the nearest neighbors of a site on one sublattice all lie on the other (*see* $Fig.1$) . Suppose initially the vacancy is at site A' which is vacant place of atom A. Here we make the basic hypothesis that : (i) in a well-ordered structure, a small number of lattice site are unoccupied, (ii) the only effective atom movements are those in which an atom jumps to a nearest neighbor unoccupied site, and (iii) the vacancies can be considered as isolated (*see* $Fig.$ 1). This vacancy migrates in such alloy as discussed by [3]. It is assumed that the jumps between the various states of these cycles represent stochastic process in which the system completely thermalizes in each state before performing the next jump [2]. In general the potential barrier height for both atomic species involved in vacancy-atom exchange process depends on the species involved in the exchange process. Hence, the potential barrier height for one type of exchange process is not the same as that for other other type of exchange process. To make the analysis moderately simple, however, we assume the potential barrier height to be the same for both atomic species involved in vacancy-atom exchange process. In other words, the potential barrier height for A type atom-vacancy exchange is assumed to be the same as that for B type atom-vacancy exchange.

In the present work the properties of six-jump cycles is discussed for low defect concentration in two-dimensions. This situation is true for a material far from the ordered-disorder transition (low concentration of structural defects). Vacancy diffuses through a direct jump or in a six-jump cycle from initial most stable state to another most stable state. Assuming the vacancy diffusion constants in both mechanisms (for one-jump and six-jump cycles) are the same, we try to compare ratio of the escape rate for the six-jump cycle to that of the the escape rate for direct jump by varying

two parameters of interest, namely, temperature and barrier height. Our analysis for the problem is based on the supersymmetric potential technique[4]-[8].

The structure of this work is as follows. In Chapter two we introduce some preliminary concepts. We divide this Chapter into two parts. Part one of the Chapter is devoted to the dynamics of vacancy motion in highly resistive limit. In part two, we introduce Supersymmetric technique that we use to address our problem. In Chapter three of section one we take a model of the energy configuration of the one-jump cycle and calculate its escape rate. Similarly in section two we see the energy configuration for the six-jump cycle and calculate its escape rate. In Chapter four, we compare the escape rates of the two mechanisms for different parameters of interest. Chapter five deals with summary and conclusion.

Chapter 2

The Dynamics for Motion of Vacany and Supersymmetric Quantum Mechanics

In preceding Chapter, we discussed vacancy diffusion in ordered alloys, which takes place by the exchange of a vacancy and an atom. In this Chapter we are going to see the equation that describes the vacancy diffusion and introduce Supersymmetric method to find the escape rate of the vacancy.

2.1 The Dynamics for Vacancy Motion

As we have seen in Chapter one, a vacancy jump between the various states of one-jump and six-jump cycles represents a stochastic process. A vacancy, an idealized particle (quasi-particle) is considered as a Brownian particle and its motion is described by Langevin equation. The Langevin equation describing the Brownian motion of a particle with mass m in a potential $U(x)$ [9], assuming that the stochastic force(term) is not affected by the potential, is given by

$$m\ddot{x} = -\gamma\dot{x} - U'(x) + f(t), \tag{2.1.1}$$

where $\dot{x}$ and $\ddot{x}$ are the first and the second time derivatives of the particle position respectively, $U'(x)$ is force due to the potential, γ is the damping constant, and $f(t)$ is the Langevin force. The Langevin force has Gaussian distribution with zero mean and with correlation function which is proportional to a δ function:

$$\begin{aligned} < f(t) >= 0, \\ < f(t), f(t') >= 2\gamma k_B T \delta(t - t'), \end{aligned} \tag{2.1.2}$$

where k_B is Boltzmann's constant and T is the temperature.

For large friction limit (large γ or, in general, short relaxation times) the variables are governed by the equation involving the slow variable only (in this case x). Fast variables are then effectively slaved by the slow variables[10], in which second order time derivative term can be neglected ($\ddot{x} \to 0$). The Langevin equation will then turn out to be

$$\gamma \dot{x} + U'(x) = f(t). \tag{2.1.3}$$

We can rewrite equation (2.1.3) as

$$dx = -\frac{1}{\gamma} U'(x) dt + \sqrt{\frac{2k_B T}{\gamma}} \xi(t) dt, \tag{2.1.4}$$

where $f(t) = \sqrt{2k_B T \gamma}\ \xi(t)$ and $\xi(t)$ is the stochastic part.

Using Ito calculus [10], for $A(x,t) = -\frac{1}{\gamma} U'(x)$, $B(x,t) = \sqrt{\frac{2k_B T}{\gamma}}$ and $dW(t) = \xi(t)dt$, the time dependent probability density $P(x,t)$ associated with the particle position in the high friction limit expressed by the equation

$$\begin{aligned} \frac{\partial P(x,t)}{\partial t} =& \frac{1}{\gamma} \frac{\partial}{\partial x} \left[U'(x) + k_B T \frac{\partial}{\partial x} \right] P(x,t) \\ =& D \frac{\partial}{\partial x} \left[\beta U'(x) + \frac{\partial}{\partial x} \right] P(x,t) \end{aligned} \tag{2.1.5}$$

is called the Smoluchoski equation(SE), where $D = \frac{k_B T}{\gamma}$ is the diffusion constant and $\beta = (k_B T)^{-1}$is the inverse temperature.

As the time doesn't explicitly occur in the SE (Eq. 2.1.5), we can make a separation $'ansatz'$ [9]

$$P(x,t) = \varphi(x)e^{-\lambda t}. \tag{2.1.6}$$

The time dependent probability distribution $P(x,t)$ will relax to time independent steady state distribution $P_s(x)$ after a very long time. Hence $P(x,t)$ will become $P_s(x)$ [10]. Thus $\frac{\partial P(x,t)}{\partial t} = 0$ implies that

$$P_s(x) = N_o e^{-\frac{\beta U(x)}{2}}. \tag{2.1.7}$$

Suppose $\varphi(x) = \phi(x)e^{-\frac{\beta U(x)}{2}}$. Then Eq. (2.1.6) can be written as

$$P(x,t) = \phi(x)e^{-\beta\frac{U(x)}{2}}e^{-\lambda t}. \tag{2.1.8}$$

Substituting the value of Eq. (2.1.8) into Eq. (2.1.5) yields time independent Schrodinger-like equation for new variable $\phi(x)$

$$-\frac{\partial^2\phi(x)}{\partial x^2} + \left(\left(\frac{\beta U'(x)}{2}\right)^2 - \frac{\beta U''(x)}{2}\right)\phi(x) = \frac{\lambda}{D}\phi(x), \tag{2.1.9}$$

where $\phi(x)$ is the eigenfunction for the Hermitian and positive semi definite Hamiltonian operator H_+ that satisfies

$$H_+\phi_n(x) = E_n^+\phi_n(x), \tag{2.1.10}$$

where $E_+^n = \frac{\lambda_n}{D}$ and $H_+ = \frac{-\partial^2}{\partial x^2} + V_+(x)$ with

$$V_+(x) = \left(\frac{\beta U'(x)}{2}\right)^2 - \frac{\beta U''(x)}{2}. \tag{2.1.11}$$

This Hamiltonian (H_+) corresponds to the motion of the particle in the potential $V_+(x)$.

For large barrier height compared to k_BT, the slowest relaxation time is the dominant quantity. Therefore escape rate λ_1 is determined by the nonzero eigenvalue, E_+^1. That is $\lambda_1 = DE_+^1$, of the SE where E_+^1 is the eigenvalue of the first excited state of Eq. (2.1.10). It would appear rather a difficult calculation is required for the evaluation of λ_1 or E_+^1 (*the eigenvalue of the first excited state*). We will show now that supersymmetry yields an easy way to determine λ_1. The eigenvalue for the first excited state E_+^1 is degenerate with the ground state ϕ_-^o of the $'$*supersymmetric partner potential*$'$ $V_-(x)$, as we shall see in section 2.2, so that $H_-\phi_o^{(-)}(x) = E_-^n\phi_o^{(-)}(x)$ with $H_- = AA^+$ and $E_-^o = E_+^1$. Therefore the problem reduced to finding the ground state eigenvalue of this $'$*partner*$'$ potential.

2.2 Supersymmetric Quantum Mechanics

Supersuymmetric method is an operator method that allows us having only the ground state wave function to construct all the excited states by acting an operators on the ground states [4] . In solving exactly for the spectrum of one dimensional potential problems, the connection between the ground state wave function and the potential is the main ingredient. Consider the time independent Schrodinger equation for a one dimensional potential problems,

$$\frac{-\hbar^2}{2m}\frac{d^2\psi(x)}{dx^2} + V(x)\psi(x) = E\psi(x), \tag{2.2.1}$$

where m is the mass, $\hbar$ is the Planck's constant, V(x) the potential, E the energy eigenvalue and $\psi(x)$ the eigenfunction. We can write Eq. (2.2.1) as

$$\hat{H}\psi = E\psi, \tag{2.2.2}$$

where $\hat{H} = \frac{-\hbar^2}{2m}\frac{\partial^2}{\partial x^2} + V(x)$.

Let us begin by assuming that we know the exact ground state solution, ψ_o for some potential $V(x)$ and the Hamiltonian $\hat{H}$. We require a knowledge of only the ground state. Let the energy of this state to be labeled by E_o. Next we define a shifted potential energy function as $V_+(x) = V(x) - E_o$, which allows us to write $Eq.$ (2.2.1) in a new form as

$$\frac{-\hbar^2}{2m}\frac{d^2\psi_o}{dx^2}(x) + V_+(x)\psi_o(x) = 0. \tag{2.2.3}$$

It follows that ψ_o satisfies the Schrodinger equation with potential $V_+(x)$ and zero ground state energy

$$H_+\psi_o = \left(\frac{-\hbar^2}{2m}\frac{d^2}{dx^2} + V_+(x)\right)\psi_o(x), \tag{2.2.4}$$

so that

$$V_+(x) = \frac{\hbar^2}{2m}\frac{\psi_o''}{\psi_o}. \tag{2.2.5}$$

This shows that based on the knowledge of the ground state wave function one can construct a global potential $V_+(x)$. Now, define a pair of operators,

$$\begin{aligned} & & A &= \tfrac{\hbar}{\sqrt{2m}}\tfrac{d}{dx} + W(x) \\ \textit{and} & & A^+ &= \tfrac{-\hbar}{\sqrt{2m}}\tfrac{d}{dx} + W(x), \end{aligned} \tag{2.2.6}$$

so that

$$H_+ = A^+A. \tag{2.2.7}$$

Substituting Eq. (2.2.6) into Eq. (2.2.7) and comparing with Eq. (2.2.4) we get

$$V_+(x) = W(x)^2 - \frac{\hbar}{\sqrt{2m}}W^{'}(x). \tag{2.2.8}$$

The quantity W(x) is usually called the "*superpotential*" for the problem. The solution for $W(x)$ in terms of the ground state wave function is

$$W(x) = \frac{-\hbar}{\sqrt{2m}}\frac{\psi_o^{'}(x)}{\psi_o(x)}. \tag{2.2.9}$$

This solution is obtained from the equation $A\psi_o = 0$ provided that we have a solution to the $H_+\psi_o = A^+A\psi_o = 0$.

By reversing the order of the operators A and A^+, we can construct a new Hamiltonian denoted by

$$H_- = AA^+ = -\frac{\hbar^2}{2m}\frac{d^2}{dx^2} + V_-(x) \tag{2.2.10}$$

where $V_-(x)$ is the new potential given as

$$V_-(x) = W(x)^2 + \frac{\hbar}{\sqrt{2m}}W^{'}(x). \tag{2.2.11}$$

The potentials $V_+(x)$ and $V_-(x)$ are known as *supersymmetric partner potentials*. That is from the energy spectra (energy eigenvalue) of their corresponding Hamiltonians, H_+ and H_- are related. The energy eigenvalues of both H_+ and H_- are positive semi-definite. To prove this connection for general superpartner potentials, we first denote the eigenfunctions of H_- and H_+ by $\psi_n^{(-)}(x)$ and $\psi_n^{(+)}(x)$ with energy eigenvalues $E_n^{(-)}$ and $E_n^{(+)}$, respectively. The integer label $n = 0, 1, 2...$ counts the number of nodes in the wave functions.

Now we need to show if $\psi_n^{(+)}(x)$ is eigenfunction of H_+ with eigenvalue $E_n^{(+)}$, and then $A\psi_n^{(+)}(x)$ is an eigenfunction of H_- with the same eigenvalue. This can be easily seen as follows:

$$H_+\psi_n^{(+)} = E_n^{(+)}\psi_n^{(+)} \tag{2.2.12}$$

and

$$\begin{aligned} H_-(A\psi_n^{(+)}) =& AA^+\left(A\psi_n^{(+)}\right) \\ =& A\left(H_+\psi_n^{(+)}\right) \\ =& E_n^{(+)}\left(A\psi_n^{(+)}\right). \end{aligned} \tag{2.2.13}$$

Similarly, if $\psi_n^{(-)}(x)$ is eigenfunction of H_- with eigenvalue $E_n^{(-)}$, then $A^+\psi_n^{(-)}(x)$ is an eigenfunction of H_+ with the same eigenvalue. That is

$$H_-\psi_n^{(-)} = E_n^{(-)}\psi_n^{(-)} \tag{2.2.14}$$

and

$$\begin{aligned} H_+(A^+\psi_n^{(-)}) =& A^+A\left(A^+\psi_n^{(-)}\right) \\ =& A^+\left(H_-\psi_n^{(-)}\right) \\ =& E_n^{(-)}\left(A^+\psi_n^{(-)}\right). \end{aligned} \tag{2.2.15}$$

One can show from Eqs. (2.2.12)-(2.2.15) and the fact that $E_o^{(+)} = 0$, if $\psi_n^{(+)}$ is an eigenfunction of H_+ with eigenvalue $E_n^{(+)}$, then $A\psi_n^{(+)}$ is an eigenfunction of H_- with the same eigenvalue, related by

$$E_n^{(-)} = E_{n+1}^{(+)}, E_o^{(+)} = 0 \tag{2.2.16}$$

$$\psi_n^{(-)} = \frac{1}{\sqrt{E_{n+1}^{(+)}}} A\psi_{n+1}^{(+)} \tag{2.2.17}$$

$$\psi_{n+1}^{(+)} = \frac{1}{\sqrt{E_n^{(-)}}} A^+\psi_n^{(-)} \tag{2.2.18}$$

where n=1,2,3,.... This connections are illustrated schematically in Fig. (2.1), from which one can see that the operators A and A^+ connect states of the same energy for

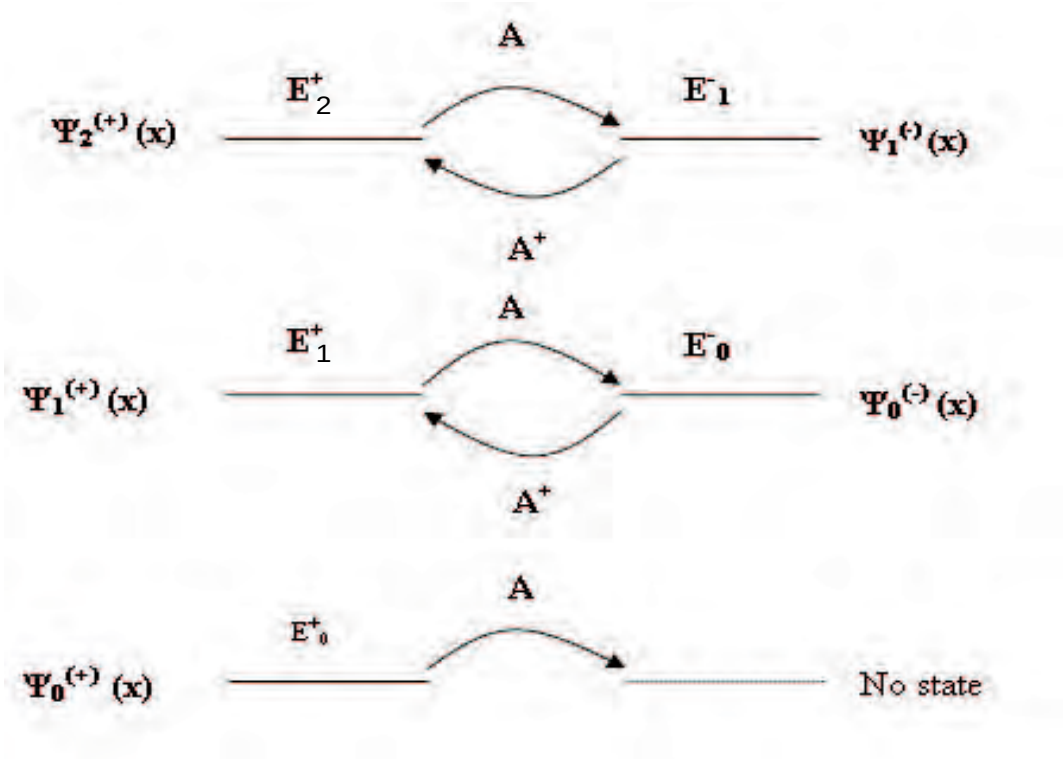

Figure 2.1: Generalized ladder operators of supersymmetric potential that connects states of the same energy.

the two. In principle, they are quite different potentialS. Notice that if $\psi_{n+1}^{(+)}\left(\psi_n^{(-)}\right)$ of $H_+\,(H_-)$ is normalized then the wave functions $\psi_n^{(-)}\left(\psi_{n+1}^{(+)}\right)$ in Eqs. (2.2.17) and (2.2.18) are also normalized. Furthermore, the operators $A(A^+)$ not only convert an eigenfunction of $H_+(H_-)$ into an eigenfunction of $H_-(H_+)$ with the same energy, but also destroys(creates) an extra node in the eigenfunction. Since the ground state wave function of H_+ is annihilated by the operator A, this state has no SUSY partner. Thus the picture we get is that knowing all the eigenfunctions of H_- using the operator A, and vice versa. Using A^+ we can construct all the eigenfunctions of H_+ from those of H_- except for the ground state.

Chapter 3

The Energy Configuration and Calculation of Escape Rate for One-Jump and Six-Jump Cycles

In Chapter two, we have seen the equation that describes a vacancy diffusion in highly resistive limit and derived the expression for the escape rate using SUSY method. In this Chapter, we will consider models for one-jump and six-jump cycles with their corresponding energy configuration to find the escape rates for vacancy to jump from one minimum state to the next.

3.1 One-Jump Cycle

3.1.1 The Energy Configuration for One-Jump Cycle

Consider $B2$ compounds to stoichiometry (low concentration structural) defect. When the atom and the vacancy exchanges their site directly (long range atom vacancy exchange), the atom crosses high potential barrier as shown in Fig. 3.1(II) thereby preserving the ordered structure. To make our model simple, we consider a piece wise linear double-well potential as shown in Fig. 3.2(I). The *supersymmetric partner potential* for $V_+(x)$, namely $V_-(x)$ is given by

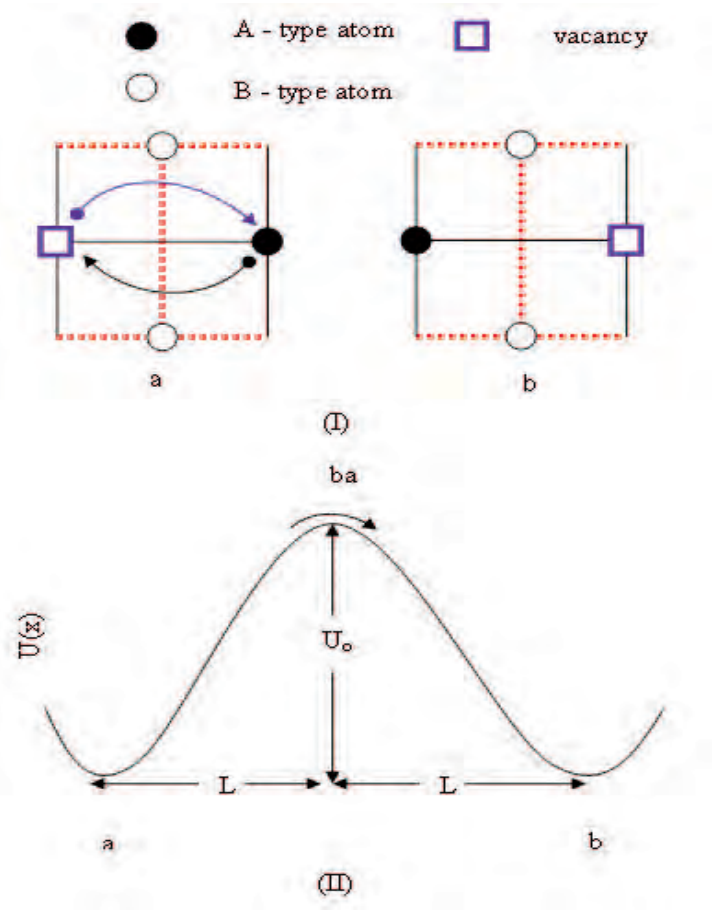

Figure 3.1: (I) The one-jump in B2 compounds. (II) Schematic picture of the energy change during one-jump cycle.

$$V_{-}(x) = \left(\frac{\beta U'(x)}{2}\right)^2 + \frac{\beta U''(x)}{2}. \tag{3.1.1}$$

For the model potential shown in Fig. (3.2), we can rewrite Eq. (3.1.1) as

$$V_{-}(x) = \left(\frac{\beta U_o}{2L}\right)^2 + 2\left(\frac{\beta U_o}{2L}\right)\left[\delta(x+L) + \delta(x-L) - \delta(x)\right]. \tag{3.1.2}$$

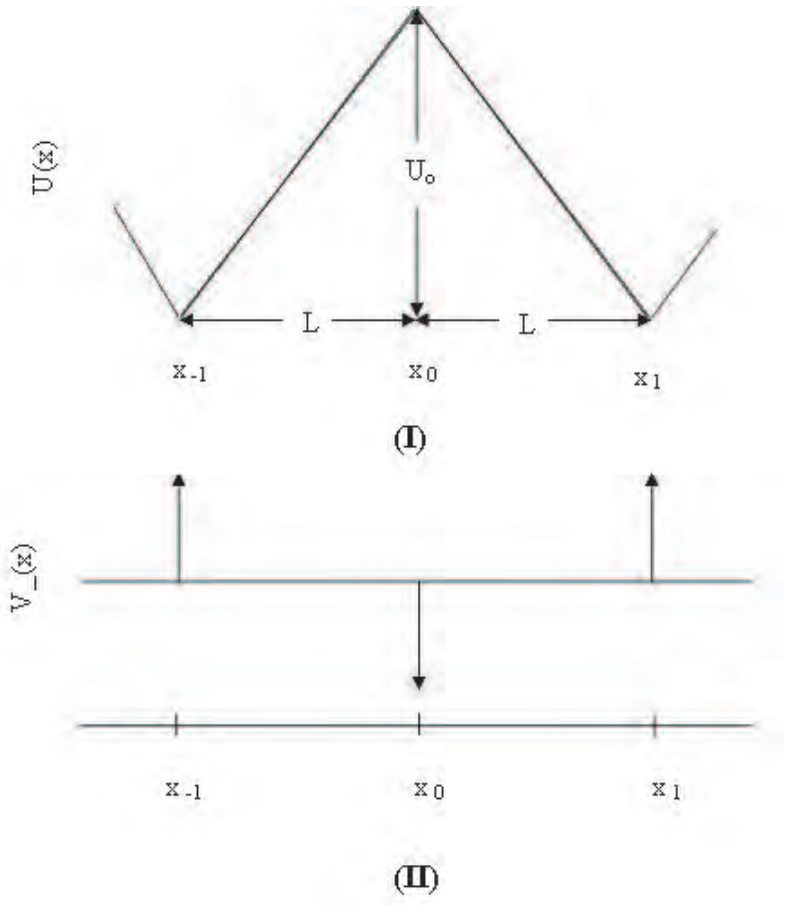

Figure 3.2: (I) The model potential U(x) versus x. (II) Plot of V_ (x) versus x (not scaled).

Defining a rescaled parameter $u_o = \frac{\beta U_o}{2}$, one can then write Eq. (3.1.2) in a simple form

$$V_{-}(x) = \left(\frac{u_o}{L}\right)^2 + 2\left(\frac{u_o}{L}\right)\left[\delta(x+L) + \delta(x-L) - \delta(x)\right]. \tag{3.1.3}$$

The Hamiltonian H_{-} is then given by

$$\begin{aligned} H_{-} &= -\frac{\partial^2}{\partial x^2} + V_{-}(x) \\ &= -\frac{\partial^2}{\partial x^2} + \left(\frac{u_o}{L}\right)^2 + 2\left(\frac{u_o}{L}\right)\left[\delta(x+L) + \delta(x-L) - \delta(x)\right]. \end{aligned} \tag{3.1.4}$$

We rescale space such that $y = \frac{x}{L}$ and substituting y into Eq. (3.1.4) leads to Hamiltonian of the form:

$$H_- = \frac{1}{L^2}\left(-\frac{\partial^2}{\partial y^2} + u_o^2 + 2u_o\left[\delta(y+1) + \delta(y-1) - \delta(y)\right]\right). \tag{3.1.5}$$

Equation (3.1.5) can be rewritten as a dimensionless Hamiltonian

$$h_- = L^2 H_- = \left(-\frac{\partial^2}{\partial y^2} + u_o^2 + 2u_o\left[\delta(y+1) + \delta(y-1) - \delta(y)\right]\right). \tag{3.1.6}$$

From Eq. (3.1.6) we have $h_-\underline{\phi^o} = \underline{e^o}\underline{\phi^o}$, where $\underline{e^o} = L^2\underline{E^o}$. From *Eq.* (2.1.10) the escape rate can then be written as

$$\lambda_{1j} = D\underline{E^o} = \frac{D\underline{e^o}}{L^2}. \tag{3.1.7}$$

3.1.2 Calculation of Escape Rate for Direct Jump

We use transfer matrix method to find the ground state energy eigenvalue of the eigenfunction $\underline{\phi^o}$. The ground state wave function $\underline{\phi^o}$ is peaked around the position of delta potential, thus the eigenfunction will have a form $Ae^{-ky} + Be^{ky}$. Assume the wave function of the form:

$$\phi_1(y) = A_1 e^{-k(y+1)} + B_1 e^{k(y+1)}, \text{for interval } y \le -1, \tag{3.1.8}$$

$$\phi_2(y) = A_2 e^{-k(y+1)} + B_2 e^{k(y+1)}, \text{for interval } -1 \le y \le 0, \tag{3.1.9}$$

$$\phi_3(y) = A_3 e^{-k(y)} + B_3 e^{k(y)}, \text{for interval } 0 \le y \le 1, \tag{3.1.10}$$

$$\phi_4(y) = A_4 e^{-k(y-1)} + B_4 e^{k(y-1)}, \text{for interval } y \ge 1 \tag{3.1.11}$$

where $k = (u_o^2 - \underline{e^o})^{\frac{1}{2}}$.

The existence of discontinuities of the first kind *i.e.*, finite jump in the potential doesn't modify the conditions of continuity imposed on the function $\underline{\phi^o}(y)$ and on its

first derivative $\frac{d\phi_-^o}{dy}$ [11]. Therefore by matching the wave function at $y=-1$ *i.e.* $\phi_2(y=-1)=\phi_1(y=-1)$, we get

$$A_2+B_2=A_1+B_1. \tag{3.1.12}$$

For a finite discontinuity of the potential that follows from Schrodinger equation, the second derivative $\frac{d^2\phi_-^o}{dy^2}$ will exhibit a finite jump. However, the integral of $\frac{d^2\phi_-^o}{dy^2}$ remains continuous [11]. Integrating the Hamiltonian h_- (Eq. 3.1.6) around $y=-1$ yields

$$\lim_{\epsilon\to 0}\int_{(y=-1-\epsilon)}^{(y=-1+\epsilon)}\left(-\frac{d^2}{dy^2}+u_o^2+[\delta(y+1)-\delta(y)+\delta(y-1)]\right)\phi_-^o(y)dy = \lim_{\epsilon\to 0}\int_{(y=-1-\epsilon)}^{(y=-1+\epsilon)}E_-^o\phi_-^o(y)dy. \tag{3.1.13}$$

Since $\phi_-^o(y)$ is continuous at any point integral of Eq. (3.1.13) reduce to

$$\lim_{\epsilon\to 0}\left(\int_{(y=-1-\epsilon)}^{(y=-1+\epsilon)}-d\phi_-^{'o}(y)+\int_{(y=-1-\epsilon)}^{(y=-1+\epsilon)}2u_o\delta(y+1)\phi_-^o(y)dy\right)=0, \tag{3.1.14}$$

where $\phi_-^{\prime o}(y)=\frac{d\phi_-^o(y)}{dy}$. Not that there is a positive delta potential of strength $2u_o$. One can simplify Eq. (3.1.14) to

$$\lim_{\epsilon\to 0}\left(\phi_-^{'o}(y=-1+\epsilon)-\phi_-^{'o}(y=-1-\epsilon)\right)=2u_o\phi_-^o(y=-1) \tag{3.1.15}$$

for

$$\lim_{\epsilon\to 0}\phi_-^{'o}(y=-1+\epsilon)=\phi_2'(y=-1), \tag{3.1.16}$$

$$\lim_{\epsilon\to 0}\phi_-^{'o}(y=-1-\epsilon)=\phi_1'(y=-1) \tag{3.1.17}$$

and

$$\lim_{\epsilon\to 0}\phi_-^o(y=-1+\epsilon)=\phi_1(y=-1)=\phi_2(y=-1) \tag{3.1.18}$$

where $\phi_2'(y=-1)=\frac{d\phi_2(y=-1)}{dy}$ and $\phi_1'(y=-1)=\frac{d\phi_1(y=-1)}{dy}$. Substituting Eqs. (3.1.16), (3.1.17) and (3.1.18) into (3.1.15) together with

$\phi_2'(y=-1) = -kA_2 + kB_2$,

$\phi_1'(y=-1) = -kA_1 + kB_1$ and

$\phi_1(y=-1) = A_1 + B_1$ these comes flowing from Eq. (3.1.8). we get

$$-A_2 + B_2 = (-1 + 2\alpha_o)\, A_1 + (1 + 2\alpha_o)\, B_1, \tag{3.1.19}$$

where $\alpha_o = \frac{u_o}{k}$.

Combining Eq. (3.1.12) and (3.1.19), we find

$$A_2 = (2 - \alpha_o)A_1 - \alpha_o B_1, \tag{3.1.20}$$

$$B_2 = \alpha_o A_1 + (1 + \alpha_o)B_1. \tag{3.1.21}$$

Using matrix transformation, we write Eqs. (3.1.20) and (3.1.21) together as

$$\begin{pmatrix} A_2 \\ B_2 \end{pmatrix} = \begin{pmatrix} (1-\alpha_o) & -\alpha_o \\ \alpha_o & (1+\alpha_o) \end{pmatrix} \begin{pmatrix} A_1 \\ B_1 \end{pmatrix} = T_1 \begin{pmatrix} A_1 \\ B_1 \end{pmatrix}, \tag{3.1.22}$$

where

$$\mathbf{T_1} = \begin{pmatrix} (1-\alpha_o) & -\alpha_o \\ \alpha_o & (1+\alpha_o) \end{pmatrix}. \tag{3.1.23}$$

The wave functions, ϕ_o^-, is continuous evrywhere, thereby matching the wave function which has the amplitudes A_2 and B_2 with the wave function having amplitudes A_3 and B_3 at $y = 0$. *i.e.* $\phi_3(y=0) = \phi_2(y=0)$, we get

$$A_3 + B_3 = A_2 e^{-k} + kB_2 e^{k}. \tag{3.1.24}$$

Integrating the Hamiltonian h_-(Eq. 3.1.6), around $y = 0$, which has a finite potential discontinuity exhibiting a finite jump for second derivative of the eigenfunction $\frac{d^2\phi_-^o}{dy^2}$[11]. Not that there is a negative delta potential of strength $2u_0$. We can get

$$\lim_{\epsilon\to 0}\left(\phi_-^{'o}(y=0+\epsilon) - \phi_-^{'o}(y=0-\epsilon)\right) = -2u_o\phi_-^o(y=0). \tag{3.1.25}$$

with

$$\lim_{\epsilon \to 0} \phi_{-}^{'o}(y = 0 + \epsilon) = \phi_3'(y = 0), \tag{3.1.26}$$

$$\lim_{\epsilon \to 0} \phi_{-}^{'o}(y = 0 - \epsilon) = \phi_2'(y = 0) \tag{3.1.27}$$

and

$$\lim_{\epsilon \to 0} \phi_{-}^{o}(y = 0 + \epsilon) = \phi_1(y = 0) = \phi_2(y = 0). \tag{3.1.28}$$

Substituting Eqs. (3.1.26 - 3.1.28), into Eq. (3.1.25) we have

$$-A_3 + B_3 = (-1 - 2\alpha_o)\, e^{-k} A_2 + (1 - 2\alpha_o)\, e^{k} B_2, \tag{3.1.29}$$

where $\alpha_o = \frac{u_o}{k}$.

From Eq. (3.1.24) and (3.1.29), we get

$$A_3 = (1 + \alpha_o) e^{-k} A_2 + \alpha_o e^{k} B_2, \tag{3.1.30}$$

$$B_3 = -\alpha_o e^{-k} A_2 + (1 - \alpha_o) e^{k} B_2. \tag{3.1.31}$$

One can write Eq. (3.1.30) and Eq. (3.1.31), using matrix transformation as

$$\begin{pmatrix} A_3 \\ B_3 \end{pmatrix} = \begin{pmatrix} (1 + \alpha_o)\, e^{-k} & \alpha_o e^{k} \\ -\alpha_o e^{-k} & (1 - \alpha_o)\, e^{k} \end{pmatrix} \begin{pmatrix} A_2 \\ B_2 \end{pmatrix} = T_2 \begin{pmatrix} A_2 \\ B_2 \end{pmatrix}, \tag{3.1.32}$$

where

$$\mathbf{T_2} = \begin{pmatrix} (1 + \alpha_o)\, e^{-k} & \alpha_o e^{k} \\ -\alpha_o e^{-k} & (1 - \alpha_o)\, e^{k} \end{pmatrix}. \tag{3.1.33}$$

Once again, comparing wave functions having the amplitudes A_3 and B_3 with the wave function having amplitudes A_4 and B_4 at $y = 1$. *i.e.* $\phi_4(y = 1) = \phi_3(y = 1)$, we obtain

$$A_4 + B_4 = A_3 e^{-k} + B_3 e^{k}. \tag{3.1.34}$$

For a finite discontinuity of the potential, integrating the Hamiltonian h_- (Eq. 3.1.6) around $y = 1$, and noting that there is a positive delta potential of strength $2u_o$, we obtain

$$\lim_{\epsilon\to 0}\left(\phi_-'^{o}(y=1+\epsilon)-\phi_-'^{o}(y=1-\epsilon)\right)=2u_o\phi_-^{o}(y)\mid_{y=1}. \tag{3.1.35}$$

For

$$\lim_{\epsilon\to 0}\phi_-'^{o}(y=1+\epsilon)=\phi_4'(y=1), \tag{3.1.36}$$

$$\lim_{\epsilon\to 0}\phi_-'^{o}(y=1-\epsilon)=\phi_3'(y=1) \tag{3.1.37}$$

and

$$\lim_{\epsilon\to 0}\phi_-^{o}(y=1+\epsilon)=\phi_4(y=1)=\phi_3(y=1). \tag{3.1.38}$$

Inserting Eqs. (3.1.36) - (3.1.38) into (3.1.35), we have

$$-A_4+B_4=(-1+2\alpha_o)\,e^{-k}A_3+(1+2\alpha_o)\,e^{k}B_3, \tag{3.1.39}$$

where $\alpha_o=\frac{u_o}{k}$. From Eq. (3.1.34) and (3.1.39) we get

$$A_4=(1-\alpha_o)e^{-k}A_3-\alpha_o e^{k}B_3, \tag{3.1.40}$$

$$B_4=\alpha_o e^{-k}A_3+(1+\alpha_o)e^{k}B_3. \tag{3.1.41}$$

From matrix transformation we write Eq. (3.1.40) and Eq. (3.1.41) as

$$\begin{pmatrix}A_4\\B_4\end{pmatrix}=\begin{pmatrix}(1-\alpha_o)\,e^{-k} & -\alpha_o e^{k}\\ \alpha_o e^{-k} & (1+\alpha_o)\,e^{k}\end{pmatrix}\begin{pmatrix}A_3\\B_3\end{pmatrix}=T_3\begin{pmatrix}A_3\\B_3\end{pmatrix}, \tag{3.1.42}$$

where

$$\mathbf{T_3}=\begin{pmatrix}(1-\alpha_o)\,e^{-k} & -\alpha_o e^{k}\\ \alpha_o e^{-k} & (1+\alpha_o)\,e^{k}\end{pmatrix}. \tag{3.1.43}$$

The transfer matrix relating the amplitudes A_4 and B_4 to the amplitude A_1 and B_1 is given by

$$\begin{pmatrix} A_4 \\ B_4 \end{pmatrix} = T_3 T_2 T_1 \begin{pmatrix} A_1 \\ B_1 \end{pmatrix} = T \begin{pmatrix} A_1 \\ B_1 \end{pmatrix}, \tag{3.1.44}$$

where $T = T_3 T_2 T_1$. Equation (3.1.44) can be rewritten with the matrix, T elements as

$$\begin{pmatrix} A_4 \\ B_4 \end{pmatrix} = \begin{pmatrix} T_{11} & T_{12} \\ T_{21} & T_{22} \end{pmatrix} \begin{pmatrix} A_1 \\ B_1 \end{pmatrix}, \tag{3.1.45}$$

where $[T]_{ij}$ for i, j $(1, 2)$ are the elements of the transfer matrix T. We can rewrite $Eq.$ (3.1.45) in a simple form:

$$A_4 = T_{11} A_1 + T_{12} B_1 \tag{3.1.46}$$

and

$$B_4 = T_{21} A_1 + T_{22} B_1. \tag{3.1.47}$$

Since we are interested in a bound state solution, the eigenfunctions for $y >> 1$ and $y << -1$ must be finite, for this we choose $B_4 = 0$ and $A_1 = 0$ respectively. Since B_1 is different from zero in Eq. (3.1.47), we see that T_{22} should be zero. It then follows that from $T = T_3 T_2 T_1$ we obtain, for T_{22}=0, the expression

$$-e^{4k} + \alpha_o^2 \left(-1 + e^{2k}\right)^2 = 0, \tag{3.1.48}$$

where $k = \sqrt{u_o^2 - e_{\underline{\ }}^o}$ and $\alpha_o = \frac{u_o}{k}$. The lowest positive solution of Eq. (3.1.48) gives us the value of $e_{\underline{\ }}^o$ when u_o is specified, then we can find the escape rate from Eq. (3.1.7) in terms of D and L.

3.2 Six-Jump Cycle

3.2.1 The Energy Configuration for Six-Jump

Unlike one-jump cycle, for $B2$ compound to stoichiometry (low concentration structural) defects, the exchange between the vacancy and the atom takes place in short range. We are interested in two dimensional well ordered binary alloy as shown Fig.

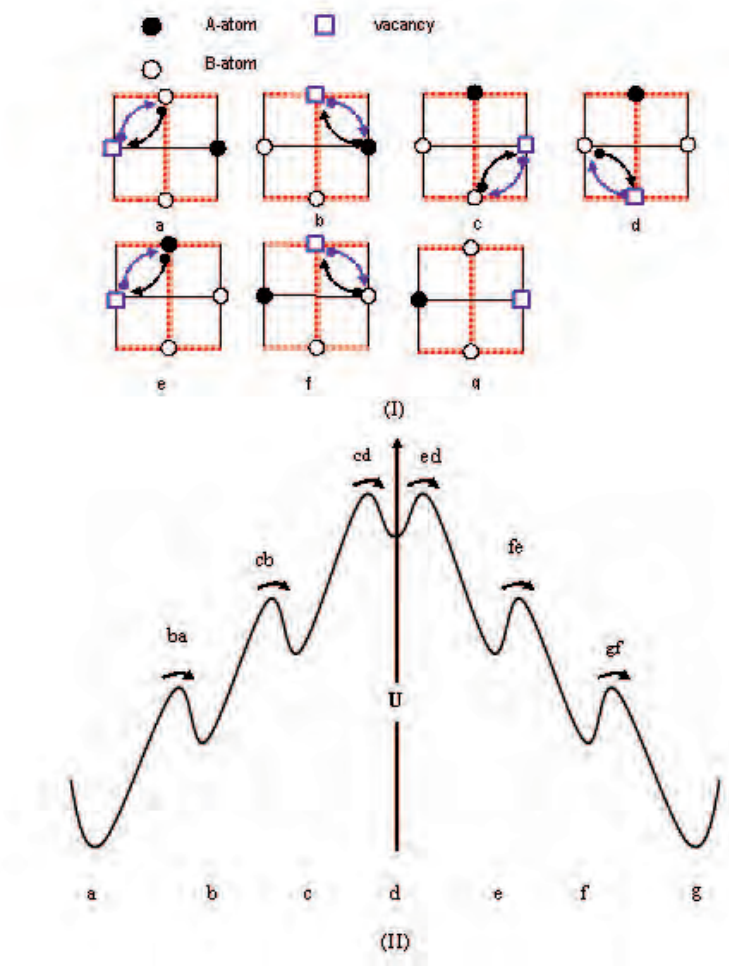

Figure 3.3: : (I) The six-jump cycles in the B2 structure. (II) A schematic picture of the energy changes of the system during the course of cycle.

1.1.

Consider the exchange of the vacancy from $A^{'}$, vacant site of A atom, with one of the nearest neighbor B atom [Fig. 3.3(I-a)]. It disorders a B atom with consequent increase in configuration energy [Fig. 3.3(I-b)]. From site B', vacant site of B atom, it jumps to one of the nearest site of A atom. As result it disorders both A and B atoms with further increase in configuration energy [Fig. 3.3(I-c)]. From site A' it jumps to one of the nearest site of B atom. In this case also it disorders two B atoms and one A atom which increases more the configuration energy [Fig.3.3(I-d)]. From site B' it jumps to nearest site of A atom which reorders one B atom with decreasing in configuration energy [Fig. 3.3(I-e)]. From site A' it jumps to nearest site of B atom. As a result it reorders an atom A, again and results in decrease the configuration energy [Fig 3.3(I-f)]. From site B' it jumps to nearest site of A atom. It further reorders atom B which decreases the configuration energy [Fig 3.3(I-g)]. By this six-jump process the first three jumps of the vacancy progressively disorder the ordered lattice and the following three jumps of the vacancy progressively re-ordered the lattice back to its initial ordered state once more. At the end the system back to its initial most stable state and ordered structure . In this process the vacant place jumps six times by a process not depending on retracing of jumps, or escape to a different stable position. Furthermore, because of the symmetry of the $B2$ structure the states are symmetric with respect to state d [Fig 3.3(II)]. Note that state a, b and c are equivalent to state g, f and e, respectively.

To make our analysis simple for model potential (see in Fig. 3.3(II)), we consider the potential profile with linear increment. We choose U_1, U_2 and the associated width a and b (shown in the Fig. 3.4(III)), such that $\frac{U_1}{a} = \frac{U_2}{b}$. This simplifies

the calculation further. Note that x_{n+1} - x_n = a + b. Introducing a dimensionless

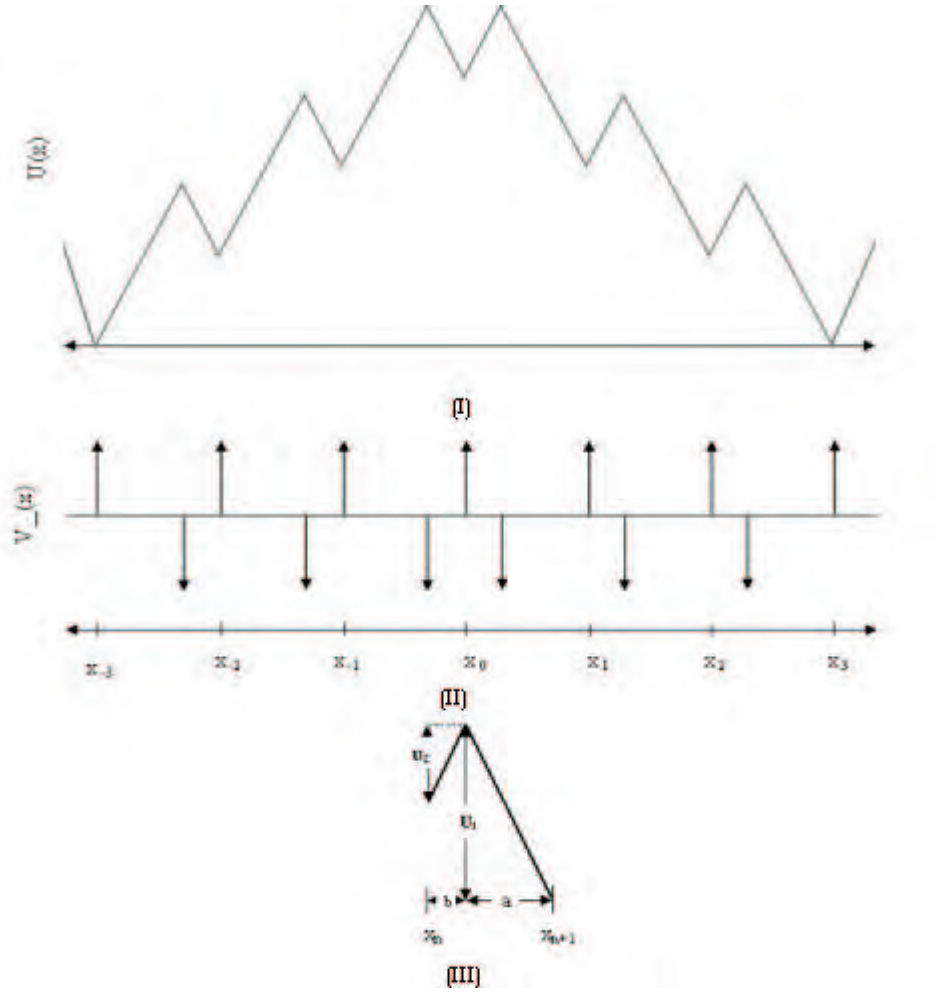

Figure 3.4: (I) The model potential U(x) versus x. (II) Plot of $V_-(x)$ versus x (not scaled). (III) A figure showing a step of the subdivided potential found between the intervals x_n and x_{n+1}.

potential $u(x) = \frac{1}{2}\beta U(x)$, the *suppersymmetric partner potential* to $V_+(x)$, namely $V_-(x)$, is then given by

$$V_-(x) = \left(\frac{\beta u'(x)}{a}\right)^2 + \frac{u''(x)}{a}. \tag{3.2.1}$$

For piecewise linear double-well potential, Equation (3.2.1) takes a simple form

$$V_{-}(x) = \left(\frac{u_1}{a}\right)^2 + \left(\frac{2u_1}{a}\right) \sum_{n=-3}^{n=3} \left[\delta(x - x_n) - \delta(x - x_n - b) - \delta(x - x_n - a)\right] \quad (3.2.2)$$

where $u_1 = \frac{1}{2}\beta U_1$. Note that the potential $V_{-}(x)$ is a series of attractive and repulsive delta-potential superimposed over a constant potential as shown in Fig. 3.4(II). Then the Hamiltonian H_{-} given by

$$H_{-} = -\frac{\partial^2}{\partial x^2} + \left(\frac{u_1}{a}\right)^2 + \left(\frac{2u_1}{a}\right) \sum_{n=-3}^{n=3} \left[\delta(x - x_n) - \delta(x - x_n - b) - \delta(x - x_n - a)\right]. \quad (3.2.3)$$

Let us rescale $x = ay$, substitute this for x in Eq. (3.2.3), the Hamiltonian is given by

$$H_{-} = -\frac{\partial^2}{a^2 \partial y^2} + \left(\frac{u_1}{a}\right)^2 + \left(\frac{2u_1}{a}\right) \sum_{n=-3}^{n=3} \left[\delta(ay - ay_n) - \delta(ay - ay_n - b) - \delta(ay - ay_n - a)\right]. \quad (3.2.4)$$

Rearranging terms we get

$$a^2 H_{-} = -\frac{\partial^2}{\partial y^2} + u_1^2 + 2u_1 \sum_{n=-3}^{n=3} \left[\delta(y - y_n) - \delta(y - y_n - b_1) - \delta(y - y_n - 1)\right], \quad (3.2.5)$$

where $b_1 = \frac{b}{a}$ and we used the property of dirac delta function $\delta(ay) = \frac{\delta(y)}{|a|}$. For $h_{-} = a^2 H_{-}$ the above Hamiltonian(Eq. (3.2.5)) can be written as

$$h_{-} = -\frac{\partial^2}{\partial y^2} + u_1^2 + 2u_1 \sum_{n=-3}^{n=3} \left[\delta(y - y_n) - \delta(y - y_n - b_1) - \delta(y - y_n - 1)\right]. \quad (3.2.6)$$

From Eq. (3.2.6) we have $h_{-}\phi_{-} = e_{-}\phi_{-}$, where $e_{-} = a^2 E_{-}$ which is a dimensionless quantity. One can then obtain the escape rate as

$$\lambda_{6j} = DE_{-} = \frac{De_{-}}{a^2}. \quad (3.2.7)$$

3.2.2 Calculation of Escape Rate for Six-Jump

Here we use transfer matrix method to find the ground state energy eigenvalue of the eigenfunction ϕ^o_-. The ground state wave function ϕ^o_- is peaked around the position of delta potential, thus eigenfunction will have a form $Ae^{-ky} + Be^{ky}$. Consider one period of the potential in the interval between y_n and y_{n+1}. Assume the wave function of the form

$$\phi_1 = A_n e^{-k(y-y_n)} + B_n e^{k(y-y_n)}, \tag{3.2.8}$$

for interval $y_n \leq y \leq y_n + b_1$, and the wave function of the form

$$\phi_2 = C_n e^{-k(y-y_n-b_1)} + D_n e^{k(y-y_n-b_1)} \tag{3.2.9}$$

for the interval $y_n + b_1 \leq y \leq y_{n+1}$, where $k = \sqrt{u_1^2 - e_-}$.

The existence of discontinuities of the first kind, *i.e.*, finite jump in the potential doesn't modify the conditions of continuity imposed on the function $\phi^o_-(y)$ and on its first derivative $\frac{d\phi^o_-}{dy}$ [11]. Therefore matching the wave function at $y = y_n + b_1$, *i.e.*, $\phi_2(y_n + b_1) = \phi_1(y_n + b_1)$, we get

$$C_n + D_n = A_n e^{-kb} + B_n e^{kb}. \tag{3.2.10}$$

For a finite discontinuity of the potential that follows from Schrodinger equation, the second derivative $\frac{d^2\phi^o_-}{dy^2}$ will exhibit a finite jump. However, the integral of $\frac{d^2\phi^o_-}{dy^2}$ remains continuous[11]. Integrating the Hamiltonian h_- (Eq. 3.2.6) around $y = y_n + b_1$ yields

$$\lim_{\epsilon \to 0} \int_{(y_n+b_1-\epsilon)}^{(y_n+b_1+\epsilon)} \left(-\frac{d^2}{dy^2} + u_1^2 + \sum_{n=-3}^{n=3} 2u_1 \left[\delta(y-y_n) - \delta(y-y_n-b_1) - \delta(y-y_n-1)\right] \right) \phi^o_-(y) dy$$

$$= \lim_{\epsilon \to 0} \int_{(y_n+b_1-\epsilon)}^{(y_n+b_1+\epsilon)} E^o_- \phi^o_-(y) dy. \tag{3.2.11}$$

Since we are integrating Eq. (3.2.11) at a point, $\phi^o_-(y)$ is continuous everywhere and noting that there is a negative delta potential of strength $2u_1$. We finally get

$$\lim_{\epsilon\to 0}\left(\int_{(y_n+b_1-\epsilon)}^{(y_n+b_1+\epsilon)} -d\phi^{'o}_-(y) + \int_{(y_n+b_1-\epsilon)}^{(y_n+b_1+\epsilon)} 2u_1\delta(y-y_n-b_1)\phi^o_-(y)dy\right) = 0, \tag{3.2.12}$$

where $\phi'^o_-(y) = \frac{d\phi^o_-(y)}{dy}$. One can simplify Eq. (3.2.12) as

$$\lim_{\epsilon\to 0}\left(\phi^{'o}_-(y_n+b_1+\epsilon) - \phi^{'o}_-(y_n+b_1-\epsilon)\right) = -2u_1\phi^o_-(y_n+b_1) \tag{3.2.13}$$

for

$$\lim_{\epsilon\to 0}\phi^{'o}_-(y_n+b_1+\epsilon) = \phi'_2(y_n+b_1), \tag{3.2.14}$$

$$\lim_{\epsilon\to 0}\phi^{'o}_-(y_n+b_1-\epsilon) = \phi'_1(y_n+b_1) \tag{3.2.15}$$

and

$$\lim_{\epsilon\to 0}\phi^o_-(y_n+b_1+\epsilon) = \phi_1(y_n+b_1) = \phi_2(y_n+b_1) \tag{3.2.16}$$

where $\phi'_2(y_n+b_1) = \frac{d\phi_2(y_n+b_1)}{dy}$ and $\phi'_1(y_n+b_1) = \frac{d\phi_1(y_n+b_1)}{dy}$.
Substituting Eqs. (3.2.14) , (3.2.15) and (3.2.16) into (3.2.13), we get

$$\phi'_2(y_n+b_1) - \phi'_1(y_n+b_1) = 2u_1\phi_1(y_n+b_1). \tag{3.2.17}$$

From Eqs. (3.2.8) and (3.2.9), we have

$$\phi'_2(y_n+b_1) = -kC_n + kD_n, \tag{3.2.18}$$

$$\phi'_1(y_n+b_1) = -kA_ne^{-kb_1} + kB_ne^{kb_1} \tag{3.2.19}$$

and

$$\phi_1(y_n+b_1) = A_ne^{-kb_1} + B_ne^{kb_1}. \tag{3.2.20}$$

Substituting Eqs. (3.2.18)-(3.2.20) in to *Eq.* (3.2.17) we find

$$-kC_n + kD_n - \left(-kA_n e^{-kb_1} + kB_n e^{kb_1}\right) = -2u_1 \left(A_n e^{-kb_1} + B_n e^{kb_1}\right). \tag{3.2.21}$$

One can rewrite Eq. (3.2.21) as

$$-C_n + D_n = (-1 - 2\alpha)\, e^{-kb_1} A_n + (1 - 2\alpha)\, e^{kb_1} B_n, \tag{3.2.22}$$

where $\alpha = \frac{u_1}{k}$.

Combining Eqs. (3.2.10) and (3.2.22), we get

$$C_n = (1 + 2\alpha)\, e^{-kb_1} A_n + \alpha e^{kb_1} B_n \tag{3.2.23}$$

$$D_n = -\alpha e^{-kb_1} A_n + (1 - \alpha)\, e^{kb_1} B_n. \tag{3.2.24}$$

Using matrix transformation we write Eqs. (3.2.23) and (3.2.24) in matrix form as

$$\begin{pmatrix} C_n \\ D_n \end{pmatrix} = \begin{pmatrix} (1+\alpha)\, e^{-kb_1} & \alpha e^{kb_1} \\ -\alpha e^{-kb_1} & (1-\alpha)\, e^{kb_1} \end{pmatrix} \begin{pmatrix} A_n \\ B_n \end{pmatrix} = T_1 \begin{pmatrix} A_n \\ B_n \end{pmatrix}, \tag{3.2.25}$$

where

$$\mathbf{T_1} = \begin{pmatrix} (1+\alpha)\, e^{-kb_1} & \alpha e^{kb_1} \\ -\alpha e^{-kb_1} & (1-\alpha)\, e^{kb_1} \end{pmatrix}. \tag{3.2.26}$$

Next, matching the wave function which have amplitudes C_n and D_n with the wave function having amplitudes A_{n+1} and B_{n+1} at $y = y_n$, *i.e.*, $\phi_1(y_n) = \phi_2(y_n)$. We obtain

$$A_{n+1} + B_{n+1} = C_n e^{-k} + kD_n e^{k}. \tag{3.2.27}$$

Integrating the Hamiltonian h_- (Eq. (3.2.6)), around $y = y_n$, having a finite potential discontinuity which exhibit a finite jump for second derivative of the eigenfunction $\frac{d^2\phi_-^o}{dy^2}$, we find that

$$\lim_{\epsilon \to 0} \int_{(y_n-\epsilon)}^{(y_n+\epsilon)} \left(-\frac{d^2}{dy^2} + u_1^2 + \sum_{n=-3}^{n=3} 2u_1 \left[\delta(y - y_n) - \delta(y - y_n - b_1) - \delta(y - y_n) - 1\right] \right) \phi_-^o(y) dy$$

$$= \lim_{\epsilon \to 0} \int_{(y_n-\epsilon)}^{(y_n+\epsilon)} E_{-}^{o} \phi_{-}^{o}(y) dy. \tag{3.2.28}$$

The eigenfunction is continuous it then follows that Eq. (3.2.28) reduced to

$$\lim_{\epsilon \to o} \int_{(y_n-\epsilon)}^{(y_n+\epsilon)} -d\phi_{-}^{'o}(y) + \int_{(y_n-\epsilon)}^{(y_n+\epsilon)} 2u_1[\delta(y - y_n - b_1)]\phi_{-}^{o}(y) dy = 0. \tag{3.2.29}$$

Not that there is a positive delta potential of strength $2u_1$, then one can reduce Eq. (3.2.29) further to

$$\lim_{\epsilon \to 0} \left(\phi_{-}^{'o}(y_n + \epsilon) - \phi_{-}^{'o}(y_n - \epsilon) \right) = 2u_1 \phi_{-}^{o}(y_n). \tag{3.2.30}$$

From *Eqs.* (3.2.8) and (3.2.9), we obtain

$$\lim_{\epsilon \to 0} \phi_{-}^{'o}(y_n + \epsilon) = \phi_1'(y_n), \tag{3.2.31}$$

$$\lim_{\epsilon \to 0} \phi_{-}^{'o}(y_n - \epsilon) = \phi_2'(y_n) \tag{3.2.32}$$

and

$$\phi_{-}^{o}(y_n) = \phi_1(y_n) = \phi_2(y_n). \tag{3.2.33}$$

Substituting *Eqs.* (3.2.31), (3.2.32) and (3.2.33) into *Eq.* (3.2.30), we get

$$\phi_1'(y_n) - \phi_2'(y_n) = 2u_1 \phi_2(y_n), \tag{3.2.34}$$

where $\phi_1'(y_n) = \frac{\phi_1(y_n)}{dy}$ and $\phi_2'(y_n) = \frac{\phi_2(y_n)}{dy}$. From equation *Eq.* (3.2.8) and (3.2.9) we get

$$\phi_1'(y_n) = -kA_n + kB_n, \tag{3.2.35}$$

$$\phi_2'(y_n) = -kC_n e^{-k} + kD_n e^{k} \tag{3.2.36}$$

and

$$\phi_2(y_n) = C_n e^{-k} + D_n e^{k} \tag{3.2.37}$$

Substituting Eqs. from (3.2.35) to (3.2.37) into (3.2.34) we find

$$-A_{n+1} + B_{n+1} = \left(-1 + \frac{2u_1}{k}\right) e^{-k} C_n + \left(1 + \frac{2u_1}{k}\right) e^{k} D_n. \tag{3.2.38}$$

For $\alpha = \frac{u_1}{k}$, one obtains

$$-A_{n+1} + B_{n+1} = (-1 + 2\alpha)\, e^{-k} C_n + (1 + 2\alpha)\, e^{k} D_n. \tag{3.2.39}$$

From Eqs. (3.2.27) and (3.2.39), we get

$$A_{n+1} = (1 - \alpha)\, e^{-ka} C_n - \alpha e^{ka} D_n, \tag{3.2.40}$$

$$B_{n+1} = \alpha e^{-k} C_n + (1 + \alpha)\, e^{k} D_n. \tag{3.2.41}$$

From matrix transformation, we rewrite Eqs. (3.2.40) and (3.2.41) as

$$\begin{pmatrix} A_{n+1} \\ B_{n+1} \end{pmatrix} = \begin{pmatrix} (1-\alpha)\, e^{-k} & -\alpha e^{k} \\ \alpha e^{-k} & (1+\alpha)\, e^{k} \end{pmatrix} \begin{pmatrix} C_n \\ D_n \end{pmatrix} = T_2 \begin{pmatrix} C_n \\ D_n \end{pmatrix}, \tag{3.2.42}$$

here

$$\mathbf{T_2} = \begin{pmatrix} (1-\alpha)\, e^{-k} & -\alpha e^{k} \\ \alpha e^{-k} & (1+\alpha)\, e^{k}. \end{pmatrix}. \tag{3.2.43}$$

The transfer matrix relating the amplitudes A_{n+1}, B_{n+1} to the amplitude A_n and B_n is given by

$$\begin{pmatrix} A_{n+1} \\ B_{n+1} \end{pmatrix} = T_2 T_1 \begin{pmatrix} A_n \\ B_n \end{pmatrix} = T \begin{pmatrix} A_n \\ B_n \end{pmatrix}, \tag{3.2.44}$$

where $T = T_2 T_1$.

The amplitudes, just after $n = 3$, A_3 and B_3 are related to the amplitudes, just after $n = 0$, A_0 and B_0 by a product of three of these transfer matrices:

$$\begin{pmatrix} A_3 \\ B_3 \end{pmatrix} = T^3 \begin{pmatrix} A_o \\ B_o \end{pmatrix}. \tag{3.2.45}$$

Eq. (3.2.45) can be rewritten element wise as

$$\begin{pmatrix} A_3 \\ B_3 \end{pmatrix} = \begin{pmatrix} [T^3]_{11} & [T^3]_{12} \\ [T^3]_{21} & [T^3]_{22} \end{pmatrix} \begin{pmatrix} A_o \\ B_o \end{pmatrix}, \tag{3.2.46}$$

where $[T^3]_{ij}$ for i, j $(1, 2)$are the elements of the transfer matrix T^3.

Once again *Eq.* (3.2.46) becomes

$$A_3 = [T^3]_{11} A_o + [T^3]_{12} B_o, \tag{3.2.47}$$

and

$$B_3 = [T^3]_{21} A_o + [T^3]_{22} B_o. \tag{3.2.48}$$

The potential shown in Fig. 3.4(I) is symmetric about $y = y_o = 0$, so that $\phi^o_-(-y) = \phi^o_-(y)$. In the interval $y_o \leq y \leq y_o + b_1$, we have Eq. (3.2.8)

$$\phi_1(y) = A_o e^{-ky} + B_o e^{ky}, \tag{3.2.49}$$

and from symmetry we get

$$\phi^o_-(-y) = \phi_1(-y) = A_o e^{ky} + B_o e^{-ky}, \tag{3.2.50}$$

in the interval $y_o - b_1 \leq y \leq y_o$. From Eqs. (3.2.49) and (3.2.50) at $y = 0$, from left and right of $y = 0$, $\phi_1(y) \mid_{y=0} = \phi_1(-y) \mid_{y=0}$, we get

$A_o + B_o = A_o + B_o$, preserves continuity for the eigen function.

Integrating the Hamiltonian h_- (Eq. 3.2.6) around $y = 0$, noting that there is positive delta potential of strenght $2u_1$. We find

$$-kA_o + kB_o - (kA_o - kB_o) = 2u_1(A_o + B_o). \tag{3.2.51}$$

Rearranging Eq. (3.2.51) we find

$$B_o = \frac{1 + \alpha}{1 - \alpha} A_o, \tag{3.2.52}$$

where $\alpha = \frac{u_1}{k}$.

Since we are intersted with a bound state, the eigenfunction for $y >> y_3$ must be finite. Hence we choose $B_3 = 0$, it then follows that from $Eq.$ (3.2.48) and from $Eq.$ (3.2.52) we get

$$[T^3]_{21}[1-\alpha] + [T^3]_{22}[1+\alpha] = 0. \tag{3.2.53}$$

From Eqs. $(A.0.20)$ and $(A.0.21)$ (see the Appendix for the derivation) we have

$$\left[T^3\right]_{21} = \frac{T_{21}\left(-d_2^3 + d_1^3\right)}{Q}, \tag{3.2.54}$$

and

$$\left[T^3\right]_{22} = \frac{\left(T_{11} - T_{22}\right)\left(-d_2^3 + d_1^3\right) + Q\left(d_2^3 + d_1^3\right)}{2Q}, \tag{3.2.55}$$

respectively. And the expressions for Q, d_1 and d_2 from Eqs. $(A.0.6)$, $(A.0.7)$ and $(A.0.8)$, respectively, are given by

$$\begin{aligned} Q &= \sqrt{(T_{11} - T_{22})^2 + 4T_{12}T_{21}}, \\ d_1 &= \frac{T_{11} + T_{22} + Q}{2}, \\ d_2 &= \frac{T_{11} + T_{22} - Q}{2}. \end{aligned}$$

T_{11}, T_{12}, T_{21} and T_{22} are elements of matrix T, which is a product of matrix T_2 (Eq. (3.2.43)) and T_1 (Eq. (3.2.26)). Then we find

$$T_{11} = (1-\alpha)(1+\alpha)e^{-k-b_1k} + \alpha^2 e^{k-b_1k}, \tag{3.2.56}$$

$$T_{12} = (1-\alpha)\alpha e^{-k+b_1k} - (1-\alpha)\alpha e^{k+b_1k}, \tag{3.2.57}$$

$$T_{21} = \alpha(1+\alpha)e^{-k-b_1k} - \alpha(1+\alpha)e^{k-b_1k} \tag{3.2.58}$$

and

$$T_{22} = \alpha^2 e^{-k+b_1k} + (1-\alpha)(1+\alpha)e^{k+b_1k} \tag{3.2.59}$$

where $k = (u_1^2 - e_-)^{\frac{1}{2}}$ and $\alpha = \frac{u_1}{k}$.

The lowest positive solution of Eq. (3.2.53) gives us the value of e_-, when u_1 and b_1 specified. Then after we can find the escape rate using Eq. (3.2.7) in terms of D and a.

Chapter 4

Result and Discussion

In Chapter three, we have got the analytical expressions for escape rates for both one-jump and six-jump cycle to go from one minimum stable state to the next stable state (*see* Fig. 3.1(I) and Fig. 3.3(I), respectively). We define the corresponding escape rates as DE^o_- and DE_- for the one-jump and six-jump cycles, respectively. The ratio R_{61} of DE_- to DE^o_- is given by

$$R_{61} = \frac{DE_-}{DE^o_-} = \frac{E_-}{E^o_-}. \tag{4.0.1}$$

From Eq. (3.2.7) and Eq. (3.1.7), we have

$$R_{61} = \frac{e_- L^2}{e^o_- a^2}. \tag{4.0.2}$$

For $L = \frac{3a}{2\sqrt{2}}$ we finally get:

$$R_{61} = \frac{9e_-}{8e^o_-}. \tag{4.0.3}$$

There are two parameters in our model, namely T, the temperature of the system, and m, which relates U, the effective total barrier height for six-jump which is equal to $2U_1$, with U_o, the barrier height of one-jump, i.e., $U_o = mU$. Holding m fixed, for different values 0.8, 1, 1.2 and 1.4, we explored the rate ratio R_{61} for a range of

temperature values. First we chose m to be 0.8, and we varied temperature keeping U_1 fixed. Figure 4.1, shows the plot of R_{61} versus $\frac{U_1}{2k_BT}$. For the whole range we

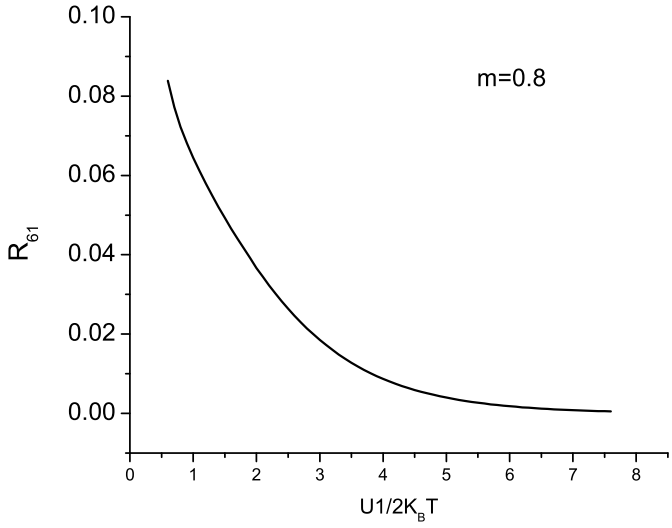

Figure 4.1: Plots of R_{61} versus $\frac{U_1}{2k_BT}$ for $m = 0.8$.

considered, the escape rate of one-jump is greater compared to the escape rate through six-jump cycle. This Shows that with the background thermal kick, the vacancy have got enough energy to cross U_o, small barrier height, easily compared to going through six-jump cycle, comparatively having larger barrier height. Within the considered temperature range, even though, one-jump is dominant its dominant nature of one-jump over the six-jump varies. At relatively high temperature limit the escape rate of six-jump is larger, taking the advantage of high thermal kick to cross the long distance (3a), as compared to relatively low temperature limit. Note as we see from Fig. 4.1, as $\frac{U_1}{2k_BT}$ go to zero R_{61} is increasing. However, we cant go beyond some limit to explore R_{61}, the reason being it is a very high temperature limit that results in

disrupting the lattice structure, in other words the alloy start melting.

When m equals to one, the effective barrier height of the six-jump is equal to that of the one-jump barrier height. The escape rate for the one-jump cycle barrier height is greater than that of the six-jump cycle. Figure 4.2 shows the plot of R_{61} versus $\frac{U_1}{k_BT}$ for $m = 1$. This shows the background thermal kick made the vacancy to cross a shorter distance ($\frac{3a}{\sqrt{2}}$), through one-jump cycle, easily than going through six-jump cycle which have got a long distance ($3a$). However, the vacancy motion is

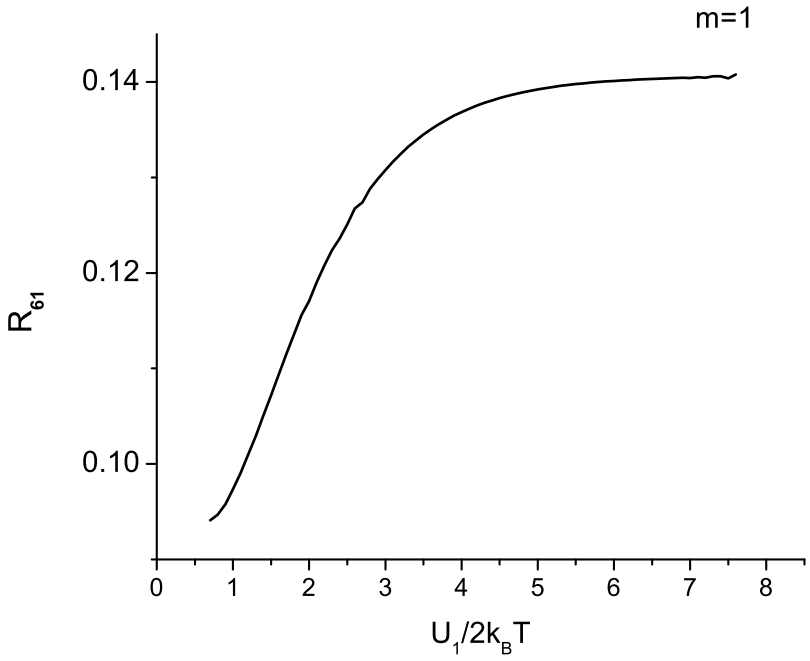

Figure 4.2: Plots of R_{61} versus $\frac{U_1}{2k_BT}$ for $m = 1$.

favored, within this temperature range, by moving a longer distance in six-jump cycle at relatively low temperature compared to one-jump.

When m greater than one $i.e$ for m : 1.2, 1.4 and 1.6, the effective total barrier height of the six-jump cycle is less than from the one-jump barrier height. The one -jump escape rate is more dominant at relatively high temperature, while the escape rate over the six-jump cycle is more dominant at relatively low temperature limit (see Fig. 4.3, 4.4, 4.5).

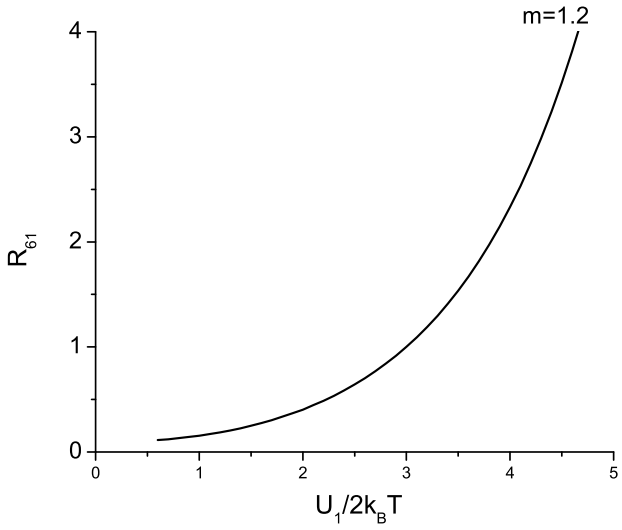

Figure 4.3: Plots of R_{61} versus $\frac{U_1}{2k_BT}$ for $m = 1.2$.

This suggests that the background thermal kick is relatively high enough at high temperature for the vacancy to cross the barrier height through one-jump cycle easily compared to the six small jump process. But at relatively low temperature limit the background thermal kick is relatively weak for the vacancy to cross the barrier through one-jump as compared to six-jump cycle, because the latter has got six small barrier heights which can be crossed with relatively small thermal kick in effect the

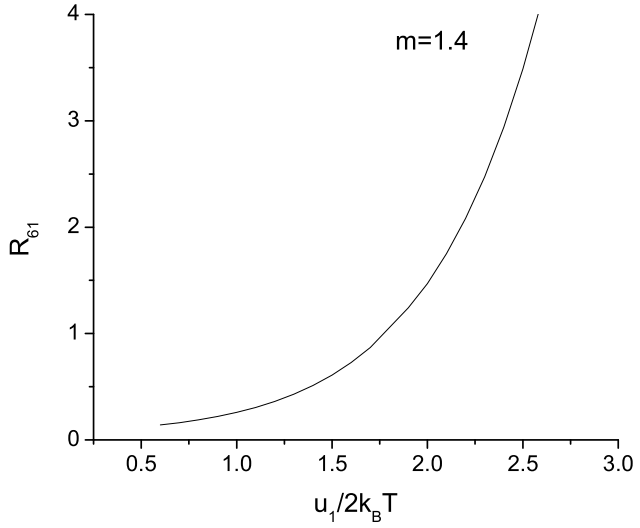

Figure 4.4: Plots of R_{61} versus $\frac{U_1}{2k_BT}$ for $m = 1.4$.

vacancy cross this barrier quickly compared to one-jump barrier height. Even if, we take the barrier height for one-jump cycle higher than the effective barrier height of six-jump cycle they show up similar properties. These are in each three cases, for m=1.2, 1.4 and 1.6, at relatively high temperature escape rate through the one-jump is greater than to that of the escape rate through six-jump cycle, in the same way at relatively low temperature the revers case observed. In all three cases there is also an interesting point (temperature) at which the escape rate through the one-jump cycle is equivalent to the escape rate through six-jump cycle, *i.e.* $R_{61} = 1$. This is the temperature at which the dominant nature of the escape rate either for one-jump or six-jump cycle changes one over the other. When $R_{61} = 1$ it indicates the vacancy has got equal chance to escape from one stable state to the next in both ways with equal escape rate. Not that the temperature at which $R_{61} = 1$ is different for different

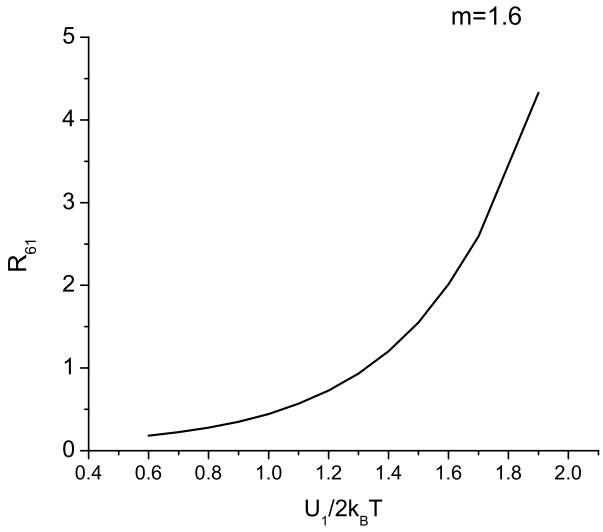

Figure 4.5: Plots of R_{61} versus $\frac{U_1}{2k_BT}$ for $m = 1.6$.

value of m. For example when $m = 1.2$ the temperature at which R_{61} equal to one is lower compared with when $m = 1.4$ or $m = 1.6$ (see the figures from 4.3-4.5). This suggest the vacancy needs relatively high background thermal kick to cross the higher barrier height than the lower.

Lastly we fix different values for $\frac{U_1}{2k_BT}$, 0.8, 1, 1.2 and 1.4, and we vary m (see Fig. 4.6, 4.7, 4.8 and 4.9, respectively). In all these cases the escape rates ratio, R_{61}, increased as m increased suggesting that the escape rate in one-jump cycle, for the fixed thermal kick, is suppressed to jump when its barrier gets higher and higher while for six-jump cycle kept the same. This shows how much the thermal kick is small, if we have relatively higher barrier for one-jump compared to six-jump cycle, the escape rate through six-jump cycle is more dominant than the one-jump cycle. Note that at certain value of m the rates ratio, R_{61} is equal to one. Showing that the

vacancy has no preference to escape either through six-jump cycle or one-jump cycle, because both has got the same escape rate. When m is below one the escape rate in one jump is more dominant.

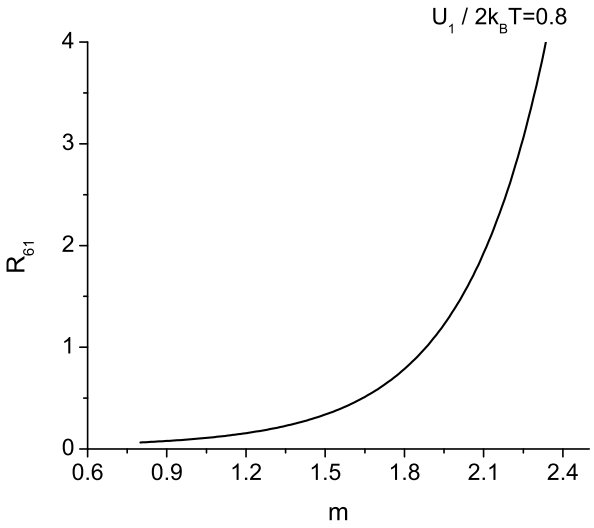

Figure 4.6: Plots of R_{61} versus m for $\frac{U_1}{2k_BT} = 0.8$.

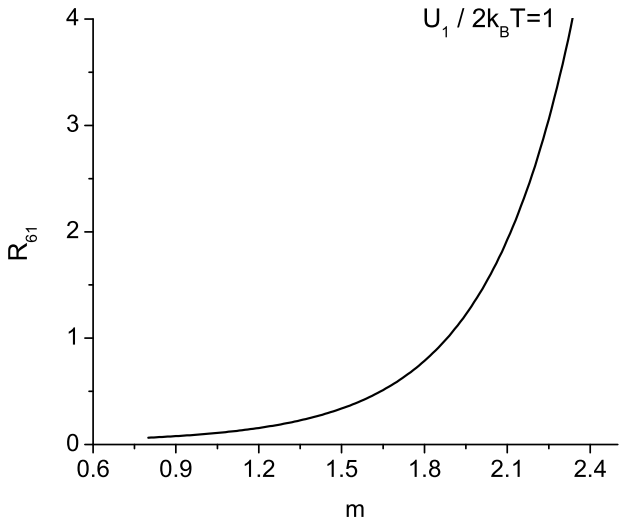

Figure 4.7: Plots of R_{61} versus m for $\frac{U_1}{2k_BT} = 1$.

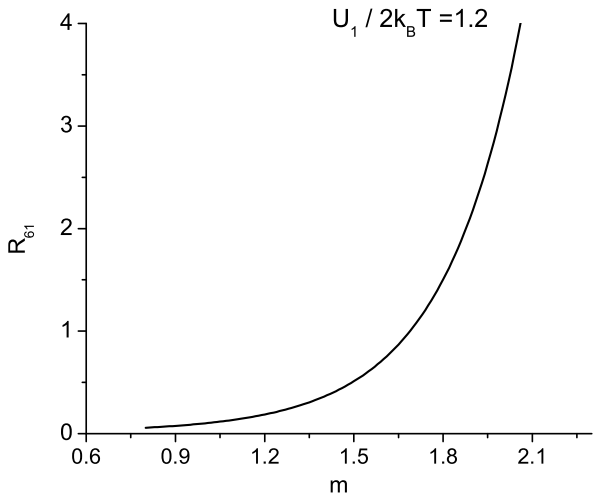

Figure 4.8: Plots of R_{61} versus m for $\frac{U_1}{2k_BT} = 1.2$.

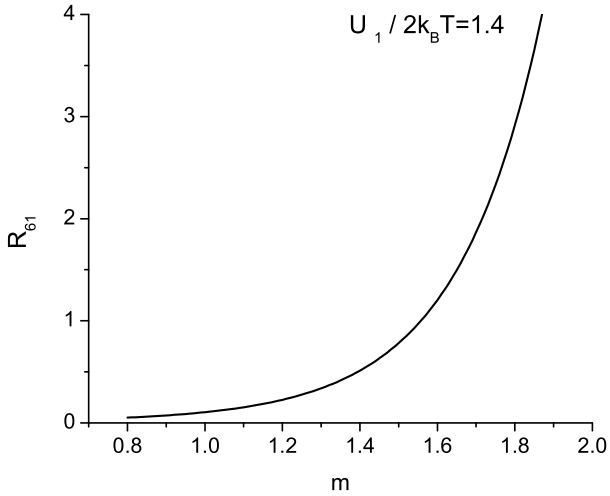

Figure 4.9: Plots of R_{61} versus m for $\frac{U_1}{2k_BT} = 1.4$.

Chapter 5

Summary and Conclusion

We have introduce a Supersymmetry Quantum Mechanics method to calculate the escape rate of vacancy in well ordered binary alloys for low concentration structural defect in two dimension. The migration is mediated by atom vacancy exchange, from initial more stable state to the next in two mechanisms. These mechanisms are long range and short range atom vacancy exchange. Using Supersymmetry Quantum Mechanics method, we analytically find the escape rate for one-jump and six-jump cycle. We compare the ratio of both one-jump and six-jump cycle escape rate by varying the barrier hight as well as temperature.

For γ less than or equal to one, the one-jump barrier height is less than or equal to the effective barrier height of six-jump cycle, the escape rate through one-jump is favored over the six-jump cycle. When the barrier height of one-jump is greater than that of effective barrier height of six-jump cycle, the escape rate becomes temperature dependent. For relatively high temperature, escape rate through one-jump cycle is higher than the six-jump cycle. However, for low temperature the escape rate through six-jump cycle is higher than the escape rate for one-jump cycle. At a ceratin temperature, the escape rate through six-jump cycle is the same as to that of

one-jump.

We have also seen that escape rate for one-jump is suppressed, when its barrier height increased keeping the effect of temperature constant. At a ceratin barrier height, the escape rate through six-jump cycle is the same as that of one-jump. Below this barrier height one-jump escape rate is dominant.

In conclusion, to make our analysis more realistic, as most alloys exist naturally, we have to consider three dimensional well ordered binary alloys at low concentration structural defect and compare the result with the experimental results and Monte Carlo simulations.

Appendix A

Derivation for Elements of the Matrix T Cubed

The explicit expression for matrix elements $[T^3]_{21}$ and $[T^3]_{22}$ can be obtained by diagonalizing the transfer matrix, using diagonalizing matrix P and P^-, then finding the cub term of T. For square matrix $n \times n$, say T in our case, we can find transforming matrix P and P^- to diagonal the matrix, D. So that $D = P^{-1}TP$ or $T = PDP^{-1}$ and from this $T^3 = PD^3P^{-1}$.

Let the diagonal element of the diagonal matrix be d_1 and d_2, *i.e.*,

$$\mathbf{D} = \begin{pmatrix} d_1 & 0 \\ 0 & d_2 \end{pmatrix}.$$

Now our task is to find P, P^{-1}, d_1 and d_2. Let the elements of the matrix T written as

$$\mathbf{T} = \begin{pmatrix} T_{11} & T_{12} \\ T_{21} & T_{22} \end{pmatrix}. \tag{A.0.1}$$

Then we write for the matrix T with its eigenvalue and eigen vector as

$$T \begin{pmatrix} X \\ Y \end{pmatrix} = d \begin{pmatrix} X \\ Y \end{pmatrix}, \tag{A.0.2}$$

where T is the square matrix and d is its corresponding eigenvalue.

Then we write Eq $(A.0.2)$ as

$$(\mathrm{T} - d\mathrm{I}) \begin{pmatrix} X \\ Y \end{pmatrix} = 0, \tag{A.0.3}$$

where I is the identity matrix and $\begin{pmatrix} X \\ Y \end{pmatrix}$ is the eigen vector.

Since the eigen vector is different from zero, its determinant coefficient must be equal to zero. Then we write it as $|T - d\ \mathrm{I}| = 0$, it then follows that

$$(T_{11} - d)(T_{22} - d) - T_{12}T_{21} = 0. \tag{A.0.4}$$

Equating for d in Eq. $(A.0.4)$ we obtain

$$d_{1,2} = \frac{(T_{11} + T_{22}) \pm \sqrt{(T_{11} - T_{22})^2} + 4T_{12}T_{21}}{2}. \tag{A.0.5}$$

Let

$$Q = \sqrt{(T_{11} - T_{22})^2 + 4T_{12}T_{21}}, \tag{A.0.6}$$

then we rewrite Eq. $(A.0.5)$ as

$$d_1 = \frac{T_{11} + T_{22} + Q}{2}, \tag{A.0.7}$$

$$d_2 = \frac{T_{11} + T_{22} - Q}{2}. \tag{A.0.8}$$

For $d = d_1$ from $Eq.$ $(A.0.3)$ and $(A.0.7)$ we rewrite as

$$\begin{pmatrix} T_{11} - \frac{1}{2}[T_{11} + T_{22} + Q] & T_{12} \\ T_{21} & T_{22} - \frac{1}{2}[T_{11} + T_{22} + Q] \end{pmatrix} \begin{pmatrix} x \\ y \end{pmatrix} = \begin{pmatrix} 0 \\ 0 \end{pmatrix},$$

Consider the second row of the above matrix, one can rewritten as

$$T_{21}x + \frac{1}{2}(T_{22} - T_{11} - Q)\, y = 0. \tag{A.0.9}$$

Choose y=1, then x will be

$$x = -\frac{T_{22} - T_{11} - Q}{2T_{21}},$$

so that

$$v_1 = (x, y) = \left(-\frac{T_{22} - T_{11} - Q}{2T_{21}}, 1\right). \tag{A.0.10}$$

For

$$d = d_2 = \frac{T_{11} + T_{22} - Q}{2},$$

from Eq. $(A.0.3)$ and $(A.0.8)$ we find

$$\begin{pmatrix} T_{11} - \frac{1}{2}[T_{11} + T_{22} - Q] & T_{12} \\ T_{21} & T_{22} - \frac{1}{2}[T_{11} + T_{22} + Q] \end{pmatrix} \begin{pmatrix} x \\ y \end{pmatrix} = \begin{pmatrix} 0 \\ 0 \end{pmatrix}. \tag{A.0.11}$$

Consider the second row

$$T_{21}x + \frac{1}{2}[T_{22} - T_{11} + Q]y = 0, \tag{A.0.12}$$

choose y=1 then x will be

$$x = -\frac{T_{22} - T_{11} + Q}{2T_{21}},$$

from this

$$v_2 = (x, y) = \left(-\frac{T_{22} - T_{11} + Q}{2T_{12}}, 1\right). \tag{A.0.13}$$

So that

$$\mathbf{P} = \begin{pmatrix} -\frac{T_{22} - T_{11} - Q}{2T_{21}} & -\frac{T_{22} - T_{11} + Q}{2T_{21}} \\ 1 & 1 \end{pmatrix}, \tag{A.0.14}$$

and P^{-1} will be

$$\mathbf{P^{-1}} = \begin{pmatrix} -\frac{T_{21}}{Q} & \frac{Q - T_{11} + T_{22}}{2Q} \\ -\frac{T_{21}}{Q} & \frac{-Q - T_{11} + T_{22}}{2Q} \end{pmatrix}. \tag{A.0.15}$$

Therefore

$$T^3 = (PDP^{-1})^3 = PD^3P^{-1}, \tag{A.0.16}$$

and we have

$$\mathbf{D^3} = \begin{pmatrix} d_1^3 & 0 \\ 0 & d_2^3 \end{pmatrix}. \tag{A.0.17}$$

Then from Eqs. $(A.0.14)$ - $(A.0.17)$ we find

$$\left[T^3\right]_{21} = \left(PD^3P^{-1}\right)_{21}, \tag{A.0.18}$$

and

$$\left[T^3\right]_{22} = \left(PD^3P^{-1}\right)_{22}. \tag{A.0.19}$$

It follows that from Eq. $(A.0.18)$

$$\left[T^3\right]_{21} = \frac{T_{21}\left(-d_2^3 + d_1^3\right)}{Q}, \tag{A.0.20}$$

and from Eq. $(A.0.19)$

$$\left[T^3\right]_{22} = \frac{\left(T_{11} - T_{22}\right)\left(-d_2^3 + d_1^3\right) + Q\left(d_2^3 + d_1^3\right)}{2Q}. \tag{A.0.21}$$

Bibliography

[1] Charles Kittel, Introduction to Solid State Physics, Seventh Edition.

[2] R. Drautz and M. Fahnle Acta mater. **47**, **No 8**, 2437, 1999.

[3] E. W Elcock and C. W. McCombie, *Phys. Rev.* **109**, 605 (1958).

[4] F. Cooper, A. Khare, U. Sukhatme, arXiv:hep-th/9405029 v2 5 May 1994.

[5] M. Bekele, G-Ananthakrishna and N. Kumar, Paramana, **46**,403 (1996).

[6] M.Bernstein and L.S. Brown, *Phys. Rev. Lett.* **52**, 1933 (1984).

[7] H. R. Jauslin, J., *Phys.* A **21**, 2337 (1988).

[8] K. Schonhammer, Z. *Phys.* B - Condensed Matter **78**, 63 (1990).

[9] H. Risken, The Fokker-Planck Equaton Methods of Solution and Applications, Second Edition, Springer-verlag, 1989, Berlin.

[10] C. W. Gardiner, Hand book of stochastic methods for physics, chemistry and natural science, Second Edition.

[11] B. H. Bransden and C. J. Joachain, Introduction to Quantum Mechanics, Second Edition.

DECLARATION

I hereby declare that this thesis is my original work and has not been presented for a degree in any other university. All sources of material used for the thesis have been duly acknowledged.

Name: ***Alemayehu Kasahun***

Signature:_____

This thesis has been submitted for examination with my approval as university advisor.

Name: ***Dr. Mulugeta Bekele***

Signature:_____

Addis Ababa University
Department of Physics
July, 2006.